NATIONAL ADVISORY COMMITTEE FOR AERONAUTICS

TECHNICAL NOTE

No. 1590

INVESTIGATION OF AN APPROXIMATELY 0.178-CHORD-THICK NACA 6-SERIES-TYPE AIRFOIL SECTION EQUIPPED WITH SEALED INTERNALLY BALANCED 0.20-CHORD AILERONS AND WITH A 0.05-CHORD TAB

By Fioravante Visconti

Langley Memorial Aeronautical Laboratory
Langley Field, Va.

Washington

May 1948

NATIONAL ADVISORY COMMITTEE FOR AERONAUTICS

TECHNICAL NOTE NO. 1590

INVESTIGATION OF AN APPROXIMATELY 0.178-CHORD-THICK NACA 6-SERIES-TYPE AIRFOIL SECTION EQUIPPED WITH SEALED INTERNALLY BALANCED 0.20-CHORD AILERONS AND WITH A 0.05-CHORD TAB

By Fioravante Visconti

SUMMARY

Hinge-moment, lift, and drag measurements were made on an approximately 0.178-chord-thick NACA 6-series-type airfoil section equipped with sealed internally balanced 0.20-chord ailerons and with a 0.05-chord tab. The purpose of this investigation was to obtain the effects of aileron contour and internal-balance chord on the aileron section hinge-moment characteristics and to determine the tab effectiveness in reducing the aileron section hinge moments.

The results of these tests indicated that increasing the aileron profile thickness from that of a true-contour to that of a straight-sided aileron would cause no significant effect on the aileron effectiveness, would increase positively the rate of change of aileron section hinge-moment coefficient with both section angle of attack and aileron deflection, and would cause little change in the hinge-moment parameter for a given rate of roll at low aileron deflection but would cause a decrease in the hinge-moment parameter for a given rate of roll at the high aileron deflections. Increasing the true-contour aileron internal-balance chord from 0 up to approximately 51 percent of the aileron chord would not cause the rate of change of aileron section hinge moment with aileron deflection to become positive. The effectiveness of the tab in reducing the aileron section hinge moments is large at low angles of attack and low aileron deflection but decreases appreciably at high aileron deflections. At the higher angles of attack, however, the tab effectiveness varies inconsistently with aileron deflection.

INTRODUCTION

Tests were conducted in the Langley two-dimensional low-turbulence tunnels for an approximate NACA 6-series-type wing section to obtain data applicable to the design of the aileron and to determine the hinge-moment effectiveness of the tab. The wing section had a maximum thickness of 0.178 chord located at station 0.35 chord and was equipped with sealed internally balanced 0.20-chord ailerons which differed in aileron contour

shape and in amount of internal balance chord. A true-contour 0.05-chord plain tab was tested in conjunction with one of the true-contour internally balanced ailerons.

Aileron section hinge-moment, aileron effectiveness, and tab hinge-moment effectiveness data were obtained at a Reynolds number of 2.5×10^6. Some tests were conducted at a Reynolds number of 6.0×10^6 to obtain the relative lift and drag characteristics of the airfoil section equipped with a true-contour neutral aileron and with a straight-sided neutral aileron.

COEFFICIENTS AND SYMBOLS

The coefficients and symbols used in this paper are as follows:

c_l	airfoil section lift coefficient $\left(\frac{l}{q_o c}\right)$
c_d	airfoil section drag coefficient $\left(\frac{d}{q_o c}\right)$
c_{h_a}	aileron section hinge-moment coefficient based on aileron chord $\left(\frac{h_a}{q_o c_a^2}\right)$
c_H	aileron section hinge-moment coefficient based on airfoil chord $\left(\frac{h_a}{q_o c^2}\right)$
$\Delta P/q_o$	seal pressure-difference coefficient, positive when pressure below seal is greater than pressure above seal
l	airfoil section lift per unit span
d	airfoil section drag per unit span
h_a	aileron section hinge moment per unit span, positive when aileron tends to deflect downward
c	airfoil section chord with aileron and tab neutral
c_a	chord of aileron behind aileron hinge axis
c_t	chord of tab behind tab hinge axis

c_b internal-balance chord, distance from aileron hinge point to midway point of flexible seal

q_o free-stream dynamic pressure $\left(\frac{1}{2}\rho_o V_o^2\right)$

ρ_o free-stream density

V_o free-stream velocity

α_o airfoil section angle of attack, degrees

δ_a aileron deflection with respect to airfoil, positive when trailing edge is deflected downward, degrees

δ_t tab deflection with respect to aileron, positive when trailing edge is deflected downward, degrees

R Reynolds number

$$c_{l_\alpha} = \left(\frac{\partial c_l}{\partial \alpha_o}\right)_{\delta_a}$$

$$c_{l_\delta} = \left(\frac{\partial c_l}{\partial \delta_a}\right)_{\alpha_o}$$

$$c_{h_\alpha} = \left(\frac{\partial c_{h_a}}{\partial \alpha_o}\right)_{\delta_a}$$

$$c_{h_\delta} = \left(\frac{\partial c_{h_a}}{\partial \delta_a}\right)_{\alpha_o}$$

$$P_\alpha = \left(\frac{\partial \frac{\Delta P}{q_o}}{\partial \alpha_o}\right)_{\delta_a}$$

$$P_\delta = \left(\frac{\partial \frac{\Delta P}{q_o}}{\partial \delta_a}\right)_{\alpha_o}$$

$c_{h_{\delta_t}} = \left(\frac{\partial c_{h_a}}{\partial \delta_t}\right)_{\alpha_o, \delta_a}$

a_δ aileron section effectiveness parameter $\left(\frac{\partial \alpha_o}{\partial \delta_a}\right)_{c_l}$

$\delta_{a_{\delta_t}}$ tab hinge-moment effectiveness parameter $\left(\frac{\partial \delta_a}{\partial \delta_t}\right)_{\alpha_o, c_h}$

$\Delta\alpha_o$ increment of airfoil section angle of attack, degrees

$(\Delta\alpha_o)_p$ effective change in angle of attack caused by rolling velocity, degrees

$\Delta\delta_a$ increment of aileron deflection, degrees

$\left(\frac{\Delta\alpha_o}{\Delta\delta_a}\right)_{\delta_a=\pm 12^\circ}$ aileron section effectiveness parameter (ratio of increment of airfoil section angle of attack to increment of aileron deflection required to maintain constant lift coefficient)

$\left(\Delta c_{h_a}\right)_\delta$ increment of aileron section hinge-moment coefficient due to aileron deflection at constant section angle of attack

$\left(\Delta c_{h_a}\right)_\alpha$ increment of aileron section hinge-moment coefficient due to change in section angle of attack at constant aileron deflection

Δc_{H_T} increment of total aileron section hinge-moment coefficient in steady roll

$\frac{\Delta c_{H_T}}{\Delta\alpha_o/\Delta\delta_a}$ aileron section hinge-moment parameter

The subscripts to partial derivatives denote the variables held constant when the partial derivatives were taken. The derivatives were measured at zero angle of attack and at zero deflection of the control surfaces except for the tab hinge-moment effectiveness parameter which was measured at zero angle of attack and zero aileron deflection

and the parameter $c_{h_{\delta_t}}$ which was measured at all the tab deflections investigated.

MODEL

The model tested was an approximate NACA 6-series-type airfoil section developed by a straight-line fairing between the NACA 63(420)-321 and NACA 65(318)-415 airfoil sections and had a 24-inch chord with its maximum thickness (0.178 chord) located at station 0.35 chord from the wing leading edge. Ordinates for the wing section are presented in table I. The model was constructed of laminated mahogany with the exception of the 0.20-chord aileron and the 0.05-chord tab, which were made of cast bronze.

The true-contour aileron, which was constructed with interchangeable internal balance, was modified by filling in the cusps on the upper and lower surfaces with modeling clay to form a straight-sided aileron. Sketches of the aileron and the aileron-tab configurations investigated are shown in figures 1 and 2, respectively. It may be noted in figure 1 that the aileron vent gaps were increased at the $0.43c_a$ internal-balance configuration; however, reference 1 shows that this slight increase is negligible. A rubber seal, attached to the aileron balance and main wing section along the complete span of the model, was used to prevent a flow of air through the aileron vent gaps. Modeling clay was used to seal the tab nose gap throughout the span of the model. The model was prepared for tests by sanding with No. 400 carborundum paper to produce aerodynamically smooth surfaces.

APPARATUS AND TESTS

When mounted in the Langley two-dimensional low-turbulence tunnels, the model completely spanned the 36-inch test sections. Aileron hinge moments were measured by means of a calibrated torque rod; whereas, the airfoil lift and drag measurements and the following correction factors, which were used to correct the tunnel data to free-air conditions, were obtained by the methods described in reference 2:

$$c_l = 0.973c_l'$$

$$c_d = 0.988c_d'$$

$$c_{h_a} = 0.988c_{h_a}'$$

$$\alpha_o = 1.015\alpha_o'$$

where the primed quantities represent the values measured in the tunnel. The hinge-moment coefficients were not corrected for tunnel-wall effects on the pressure distribution over the airfoil; approximate calculations, however, indicate that the correction probably does not exceed $0.002c_l'$.

The airfoil-lift and aileron hinge-moment data were obtained at aileron and tab deflections ranging from -18° to 12° and -20° to 20°, respectively, at a Reynolds number of 2.5×10^6 corresponding to a Mach number of 0.17. For the aileron-neutral condition, relative lift and drag characteristics of the airfoil section equipped with the true-contour aileron and with the straight-sided aileron were obtained in the Langley two-dimensional low-turbulence pressure tunnel at a Reynolds number of 6.0×10^6 corresponding to a Mach number of 0.12.

RESULTS AND DISCUSSION

Aileron Characteristics

Airfoil-lift, airfoil-drag, and aileron hinge-moment data applicable to the design of the aileron are presented in figures 3 to 11, and a summary of the parameters used in this investigation is presented in table II. The discussion of the data refers to the data obtained at a Reynolds number of 2.5×10^6 unless otherwise stated.

Section characteristics.- The aileron-contour modification resulted in a reduction of approximately 3 percent in c_{l_α} for the two Reynolds number investigated (figs. 3 to 5 and table II) and caused no significant change in maximum section lift coefficient or minimum section drag coefficient at a Reynolds number of 6.0×10^6. A negligible decrease in lift-curve slope occurred with a change in Reynolds number regardless of the aileron contour investigated.

Increasing the aileron profile from a true-contour aileron to a straight-sided aileron had no substantial effect on the parameters c_{l_δ} and α_δ (figs. 4 and 5 and table II). The values of the effectiveness parameter α_δ (table II) of the two ailerons investigated with $0.43c_a$ internal balance were approximately 0.88 percent of the value (-0.55) predicted from thin airfoil theory in reference 3 and were approximately equal to the value obtained for the NACA 65_3-418 airfoil equipped with a plain true-contour 0.20-chord aileron (reference 4). At a section lift coefficient of 0.40, the values of the effectiveness parameter $\left(\frac{\Delta\alpha_o}{\Delta\delta_a}\right)_{\delta_a=\pm 12^\circ}$ (table II) indicated that no change in aileron

effectiveness occurs over the range of aileron deflection of ±12° for the ailerons of different contour equipped with $0.43c_a$ internal balance.

A change in the aileron contour from a true-contour aileron to a straight-sided aileron with $0.43c_a$ internal balance increased positively the values of c_{h_δ} and c_{h_α} from −0.0031 to −0.0021 and from −0.0034 to −0.0011, respectively (fig. 9). A decrease in the sealed internal-balance chord from $0.60c_a$ to $0.43c_a$ increased negatively the value of the parameter c_{h_δ} from 0.0028 to −0.0031 and had a relative smaller effect (−0.0014 to −0.0034) on c_{h_α}. Values of the parameters c_{h_δ} and c_{h_α} of the true-contour aileron with less than $0.43c_a$ internal balance were computed from the following equations:

$$c_{h_{\delta_1}} = c_{h_{\delta_2}} + \frac{P_\delta}{2}\left[\left(\frac{c_b}{c_a}\right)_1^2 - \left(\frac{c_b}{c_a}\right)_2^2\right] \tag{1}$$

$$c_{h_{\alpha_1}} = c_{h_{\alpha_2}} + \frac{P_\alpha}{2}\left[\left(\frac{c_b}{c_a}\right)_1^2 - \left(\frac{c_b}{c_a}\right)_2^2\right] \tag{2}$$

where the subscripts 1 and 2 denote any given amount of internal balance. Data for the three internally balanced true-contour ailerons were substituted in equations (1) and (2), and average values of c_{h_δ} and c_{h_α} of ailerons with less than $0.43c_a$ internal balance are plotted in figure 9. Increasing the true-contour aileron internal-balance chord from 0 up to approximately 51 percent of the aileron chord would not cause the rate of change of aileron section hinge moments with aileron deflection to become positive and would have a relatively smaller effect on the rate of change of aileron section hinge moments with section angle of attack.

Effect of contour on characteristics in steady roll.- For comparison of the ailerons of different contours, the rate of change of the total aileron section hinge-moment coefficient with aileron deflection in steady roll was calculated by the equation given in reference 5

$$\Delta c_{H_T} = \left(\frac{c_a}{c}\right)^2 \left\{ \left(\Delta c_h\right)_\delta \left[1 - \frac{n\left(\Delta c_h\right)_\alpha}{\left(\Delta\alpha_o/\Delta\delta_a\right)\left(\Delta c_h\right)_\delta} \right] \right\} \qquad (3)$$

where $n = \frac{2\left(\Delta\alpha_o\right)_p}{\Delta\delta_a}$. Values of $\frac{2\left(\Delta\alpha_o\right)_p}{\Delta\delta_a}$ of 0.29 and 0.28 were obtained from the data of reference 6 for corresponding values of $\frac{\Delta\alpha_o}{\Delta\delta_a}$ of the true-contour and straight-sided ailerons, respectively. These values were calculated for a typical large airplane which has the following characteristics:

Aileron chord (constant percent of wing chord)	20.0
Aileron location, fraction of semispan:	
Inboard end	0.541
Outboard end	0.990
Wing aspect ratio	9.0
Wing taper ratio	0.379

An equal up and down aileron deflection is assumed in this method of analysis.

The hinge-moment parameter $\frac{\Delta c_{H_T}}{\Delta\alpha_o/\Delta\delta_a}$ plotted against $\Delta\alpha_o$ (fig. 11) is used for comparison of ailerons of different contour. The smaller the value of the hinge-moment parameter $\frac{\Delta c_{H_T}}{\Delta\alpha_o/\Delta\delta_a}$ for a given value of $\Delta\alpha_o$, the more advantageous the combination should be for providing a lower control force for a given helix angle of the wing tip. Increasing the true-contour-aileron profile thickness to form a straight-sided aileron would cause little change in the hinge-moment parameter $\frac{\Delta c_{H_T}}{\Delta\alpha_o/\Delta\delta_a}$ for a given rate of roll at low aileron deflections but would cause a decrease in the hinge-moment parameter for a given rate of roll at the high aileron deflection. Within a range of aileron deflection of 0° to −6°, the control forces of the true-contour aileron with $0.43c_a$ internal balance would be approximately the same as those of the straight-sided aileron with $0.43c_a$ internal balance.

Tab Characteristics

The discussion of the tab characteristics refers to the data presented in figures 12 to 14 which were obtained at a Reynolds number of 2.5×10^6.

At low angles of attack (-3° to 3°), the rate of change of the aileron section hinge-moment coefficient with aileron deflection for low aileron deflections becomes gradually more negative as the tab is deflected upwards and gradually less negative as the tab is deflected downward. (See fig. 12.) The rate of change of aileron section hinge-moment coefficient with aileron deflection for low aileron deflections remains reasonably constant at the high angle of attack of 10.2°. The rate of change of aileron hinge moment with tab deflection is presented in figure 13 for the aileron neutral, which is the condition of most importance for trimming. The tab appears to be most effective in reducing the aileron section hinge moments at the low angles of attack between a range of tab deflection of -15° to 10°. At the higher angles of attack, a reduction occurs in the tab trimming effectiveness.

The rate of change of aileron deflection with tab deflection $\delta_{a_{\delta_t}}$ is a measure of the effectiveness of the tab in balancing the increment of aileron hinge moment caused by the aileron deflection at a constant angle of attack. The tab effectiveness parameter $\delta_{a_{\delta_t}}$ indicates that the smaller the tab deflection required to balance the increment of aileron hinge moment due to a given aileron deflection, the greater is the tab hinge-moment effectiveness. The value of $\delta_{a_{\delta_t}}$ measured at zero angle of attack and at zero aileron deflection (fig. 14) is maximum and equal to approximately 2.7 for a very limited range of aileron deflection between approximately -4° to 4°; however, the tab retains most of this effectiveness in the range of aileron deflection from -8° to 6°. The effectiveness of the tab in reducing the aileron section hinge moments is large at low angles of attack and low aileron deflections but decreases appreciably at high aileron deflections. At the higher angles of attack, however, the tab effectiveness varies inconsistently with aileron deflection.

CONCLUSIONS

An investigation made on an approximately 0.178-chord-thick NACA 6-series-airfoil section equipped with 0.20-chord ailerons and with a 0.05-chord tab indicates the following conclusions:

1. Increasing the true-contour aileron profile thickness to form a straight-sided aileron would cause

   (a) No significant effect on the aileron section effectiveness parameter α_δ

   (b) A positive increase in the rate of change of aileron section hinge-moment coefficient with both section angle of attack and aileron deflection

(c) Little change in the aileron section hinge-moment parameter for a given rate of roll at low aileron deflection, but a decrease in this hinge-moment parameter for a given rate of roll at the high aileron deflections

(d) A slight decrease in the rate of change of section lift coefficient c_l with section angle of attack α_o

(e) Little affect on the maximum section lift coefficient and the section drag coefficients throughout the low drag range for a neutral aileron

2. Increasing the true-contour aileron sealed internal-balance chord from 0 up to approximately 51 percent of the aileron chord would

(a) Not cause the rate of change of aileron section hinge moments with aileron deflection c_{h_δ} to become positive

(b) Have a relatively smaller effect on the rate of change of aileron section hinge moments with section angle of attack c_{h_α}

3. The effectiveness of the tab in reducing the aileron section hinge moments is large at low angles of attack and low aileron deflections but decreases appreciably at high aileron deflections. At the higher angles of attack, however, the tab effectiveness varies inconsistently with aileron deflection.

Langley Memorial Aeronautical Laboratory
National Advisory Committee for Aeronautics
Langley Field, Va., December 9, 1947

REFERENCES

1. Denaci, H. G., and Bird, J. D.: Wind-Tunnel Tests of Ailerons at Various Speeds. II - Ailerons of 0.20 Airfoil Chord and True Contour with 0.60 Aileron-Chord Sealed Internal Balance on the NACA 66,2-216 Airfoil. NACA ACR No. 3F18, 1943.

2. von Doenhoff, Albert E., and Abbott, Frank T., Jr.: The Langley Two-Dimensional Low-Turbulence Pressure Tunnel. NACA TN No. 1283, 1947.

3. Ames, Milton B., Jr., and Sears, Richard I.: Determination of Control-Surface Characteristics from NACA Plain-Flap and Tab Data. NACA Rep. No. 721, 1941.

4. Braslow, Albert L: Wind-Tunnel Investigation of Aileron Effectiveness of 0.20-Airfoil-Chord Plain Ailerons of True Airfoil Contour on NACA 65_2-415, 65_3-418, and 65_4-421 Airfoil Sections. NACA CB No. L4H12, 1944.

5. Underwood, William J., Braslow, Albert L., and Cahill, Jones F.: Two-Dimensional Wind-Tunnel Investigation of 0.20-Airfoil-Chord Plain Ailerons of Different Contour on an NACA 65_1-210 Airfoil Section. NACA ACR No. L5F27, 1945.

6. Langley Research Department: Summary of Lateral-Control Research. (Compiled by Thomas A. Toll.) NACA TN No. 1245, 1947.

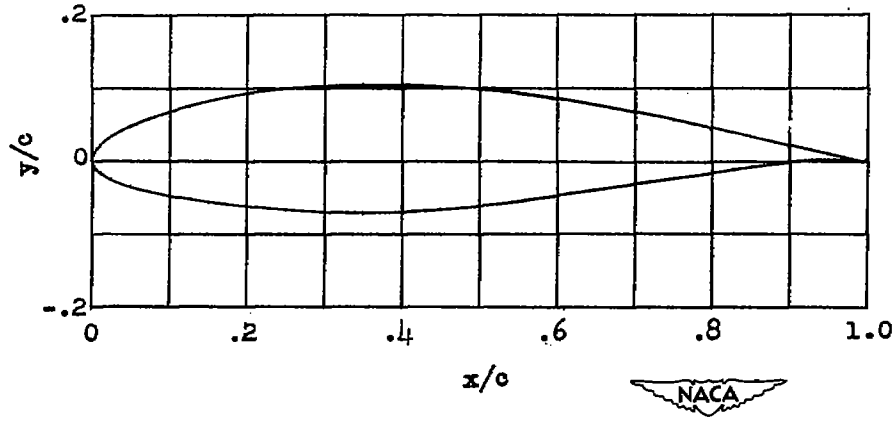

TABLE I

ORDINATES FOR AN APPROXIMATE 0.178-CHORD-THICK NACA 6-SERIES-TYPE AIRFOIL SECTION

[Stations and ordinates given in percent of airfoil chord]

Station	Upper ordinate	Lower ordinate
0	0	0
.155	1.24	-.527
.50	1.83	-1.08
1	2.36	-1.57
2.5	3.49	-2.52
5	4.85	-3.48
7.5	5.96	-4.20
10	6.87	-4.81
12.5	7.63	-5.29
15	8.29	-5.74
20	9.27	-6.39
25	9.93	-6.81
30	10.42	-7.07
35	10.67	-7.14
40	10.64	-7.05
45	10.42	-6.71
50	10.00	-6.26
55	9.42	-5.66
60	8.68	-4.97
65	7.81	-4.23
70	6.81	-3.40
75	5.71	-2.54
80	4.54	-1.71
85	3.33	-.93
90	2.12	-.28
95	.98	.15
100	0	0
L.E. radius: 2.20 Slope of radius through L.E.: 0.162		

TABLE II.- SECTION PARAMETERS MEASURED AT $\alpha_o = 0^\circ$ AND $\delta_a = 0^\circ$ EXCEPT FOR $\left(\frac{\Delta\alpha_o}{\Delta\delta_a}\right)_{\delta_a=\pm12^\circ}$

MEASURED AT $c_l = 0.40$

Internal balance	R	c_{l_α}	c_{l_δ}	α_δ	$\left(\frac{\Delta\alpha_o}{\Delta\delta_a}\right)_{\delta_a=\pm12^\circ}$	c_{h_α}	c_{h_δ}
True-contour aileron							
$0.60c_a$	2.5×10^6	-----	-----	------	----------	-0.0014	0.0028
$0.50c_a$	2.5	-----	-----	------	----------	-.0025	-.0005
$0.43c_a$	2.5	0.117	0.055	-0.480	-0.480	-.0034	-.0031
	6.0	.116	-----	------	----------	-------	-------
Straight-sided aileron							
$0.43c_a$	2.5	0.113	0.055	-0.485	-0.480	-0.0011	-0.0021
	6.0	.112	-----	------	----------	-------	-------

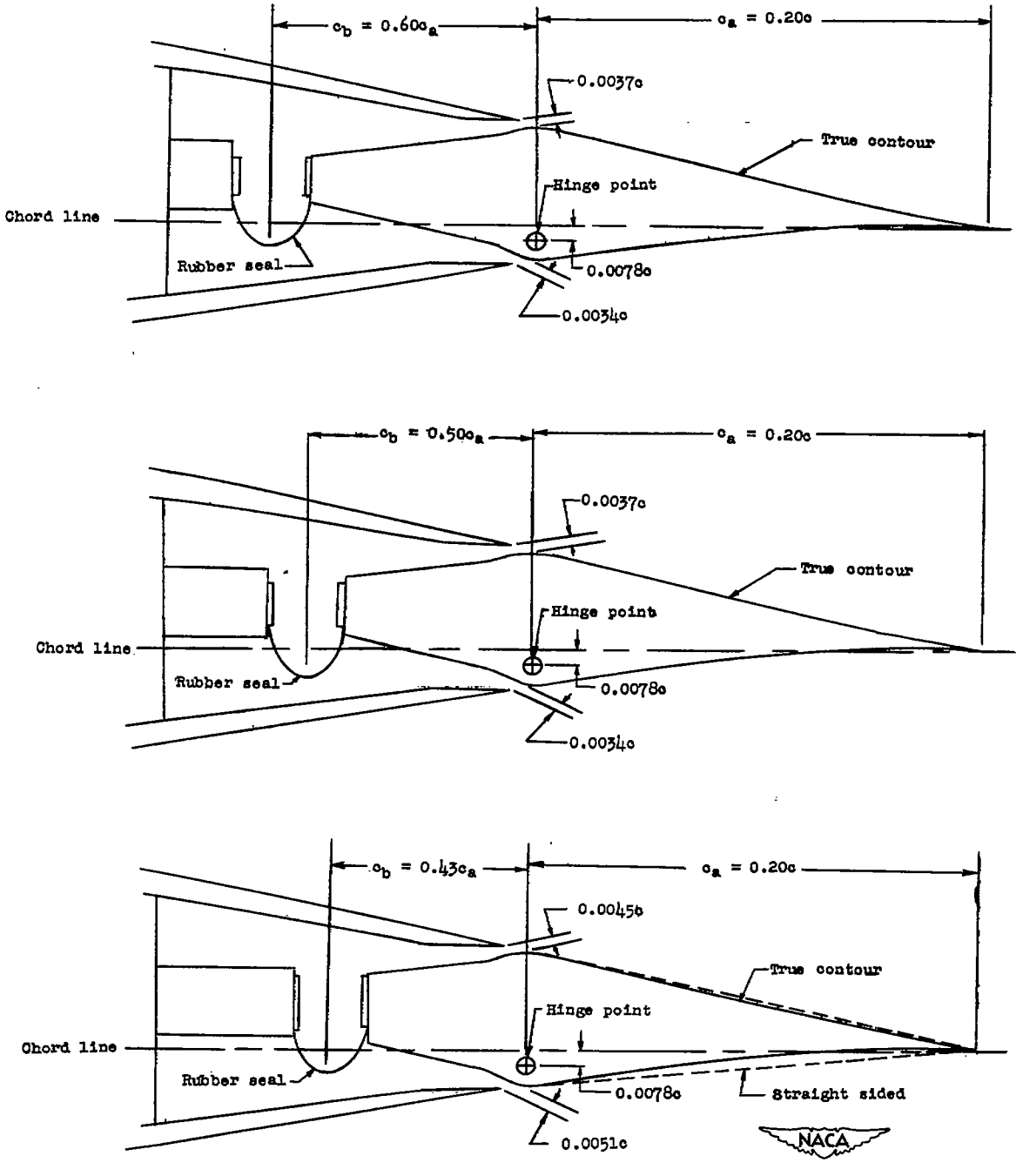

Figure 1.- Sketch of the internally balanced aileron configuration tested on an approximate 0.178-chord-thick NACA 6-series-type airfoil section.

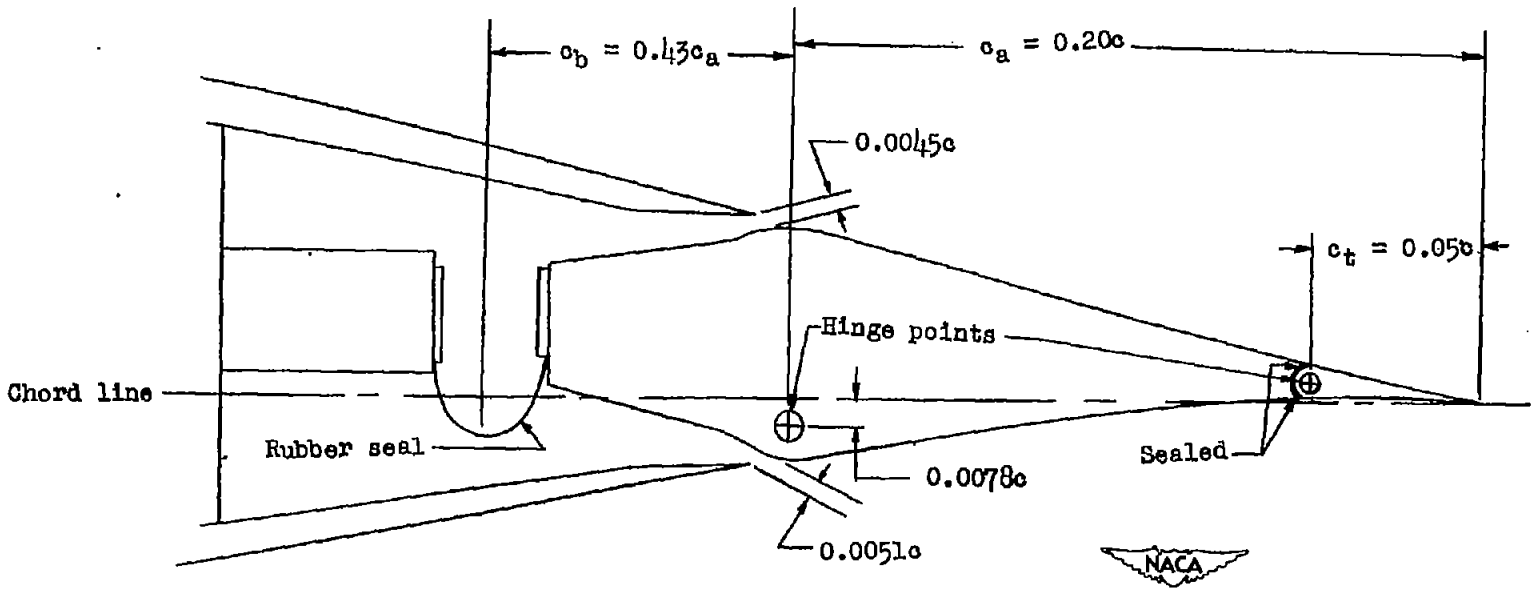

Figure 2.- Sketch of the internally balanced true-contour aileron equipped with a tab tested for an approximate 0.178-chord-thick NACA 6-series-type airfoil section.

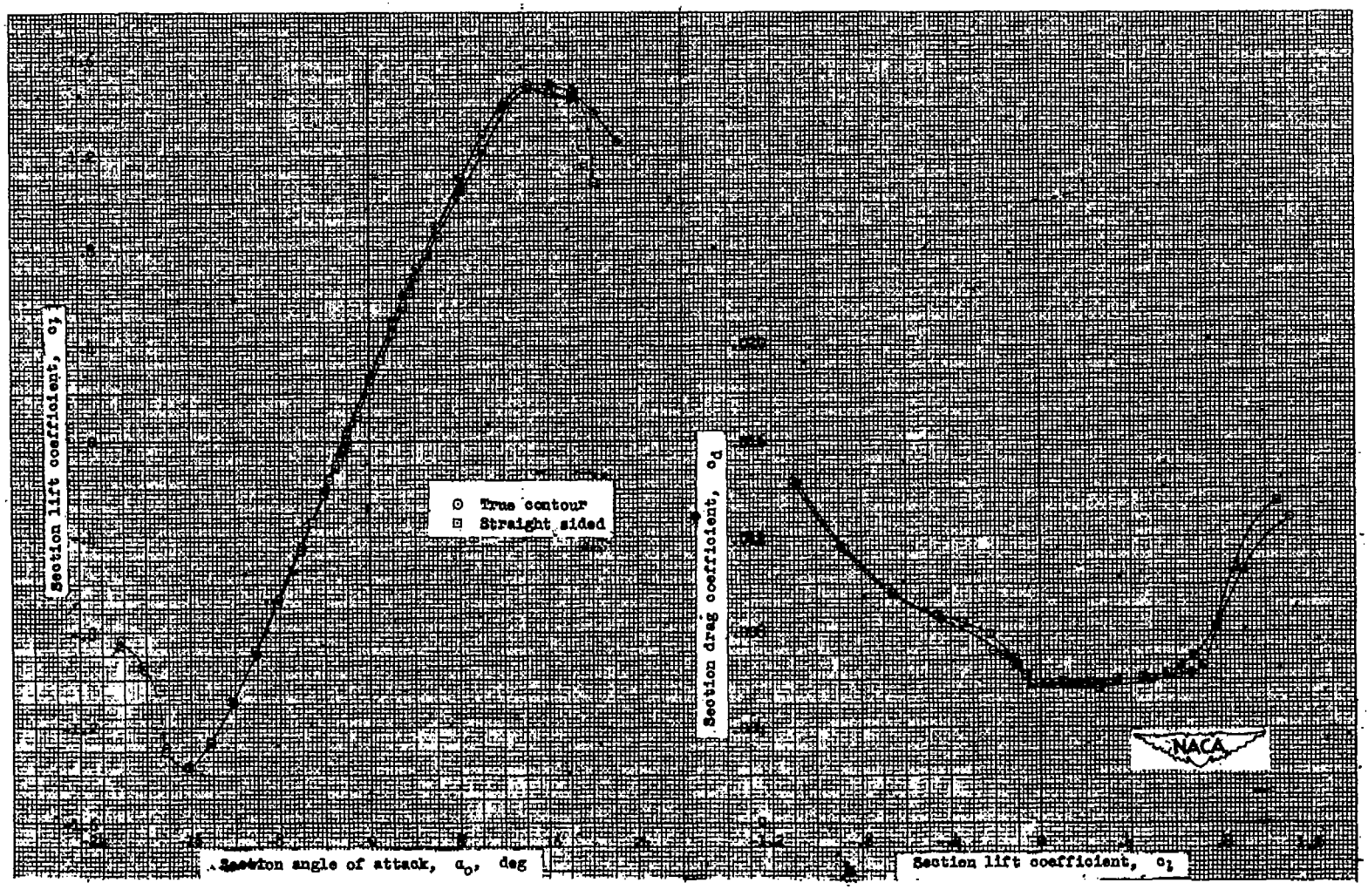

Figure 3.- Comparison of section lift and drag characteristics of an approximate 0.178-chord-thick NACA 6-series-type airfoil section equipped with differently shaped 0.20-chord ailerons with sealed 0.43-aileron-chord internal balance. δ_a, 0°; R, 6.0×10^6.

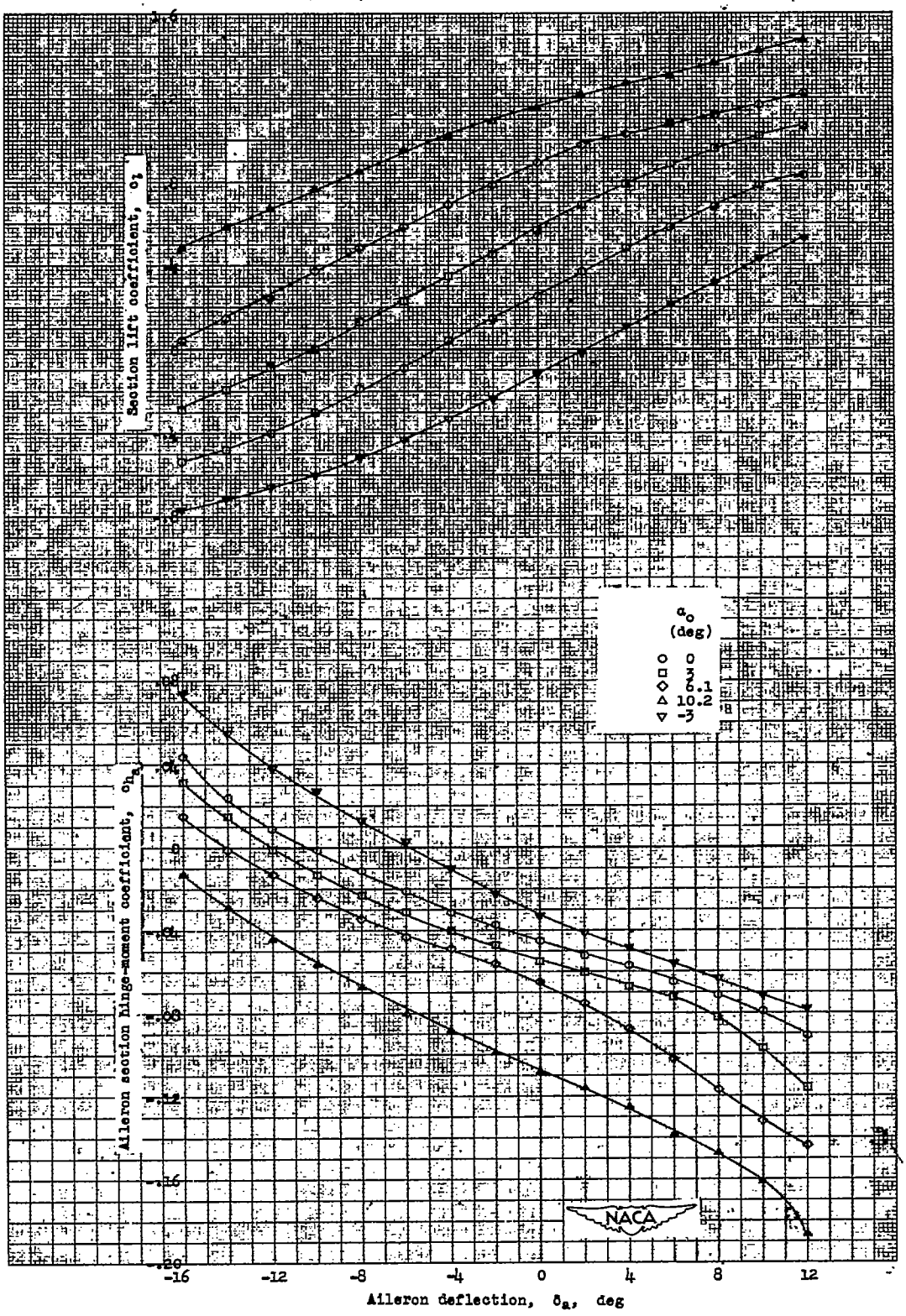

Figure 4.- Aileron effectiveness and hinge-moment characteristics of the 0.20-chord true-contour aileron with a sealed 0.45-aileron-chord internal balance on an approximate 0.175-chord-thick NACA 6-series-type airfoil section. R, 2.5 x 10^6.

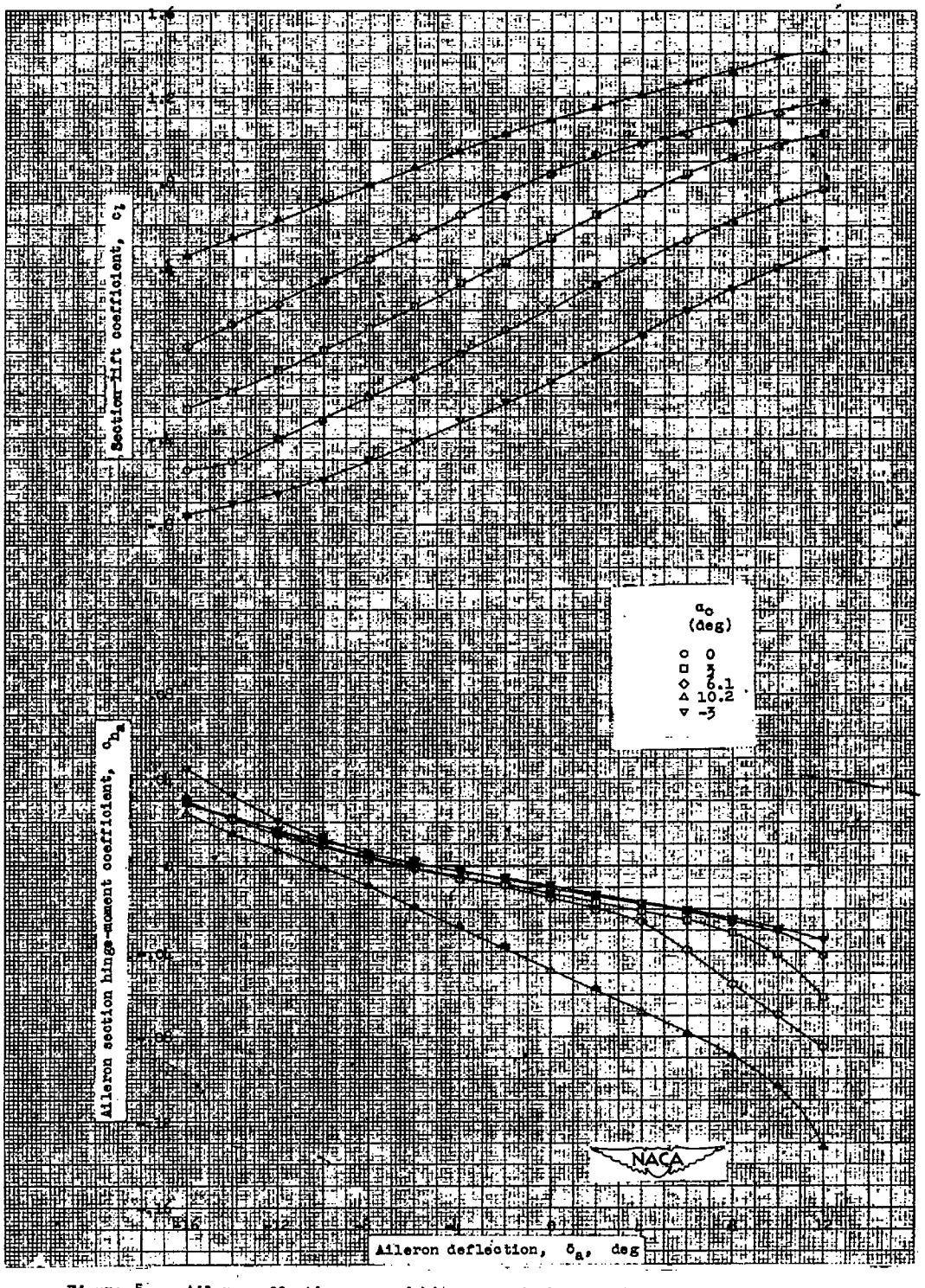

Figure 5.- Aileron effectiveness and hinge-moment characteristics of the 0.20-chord straight-sided aileron with a sealed 0.43-aileron-chord internal balance on an approximate 0.178-chord-thick NACA 6-series-type airfoil section. R, 2.5×10^6.

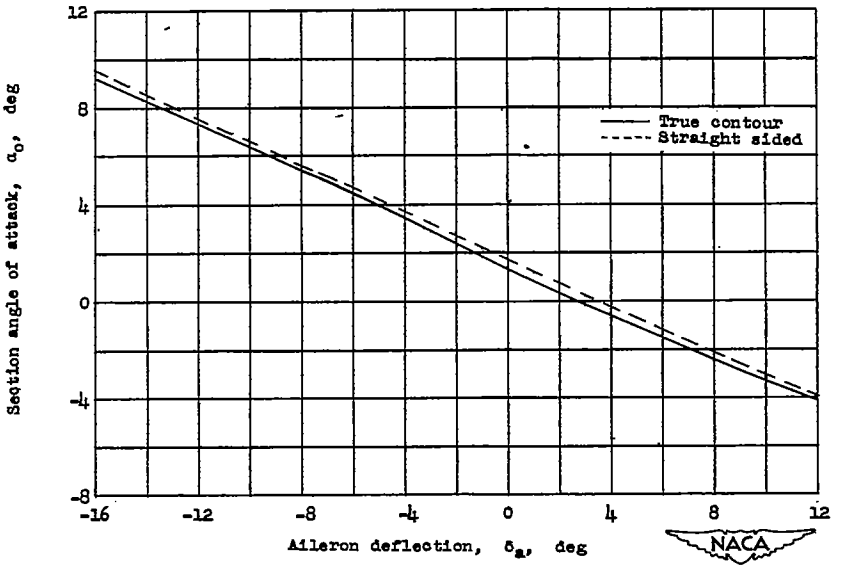

Figure 6.- Variation of section angle of attack with aileron deflection at a constant section lift coefficient of 0.40 on an approximate 0.178-chord-thick NACA 6-series-type airfoil section for two differently shaped 0.20-chord ailerons with sealed 0.43-aileron-chord internal balance. R, 2.5×10^6.

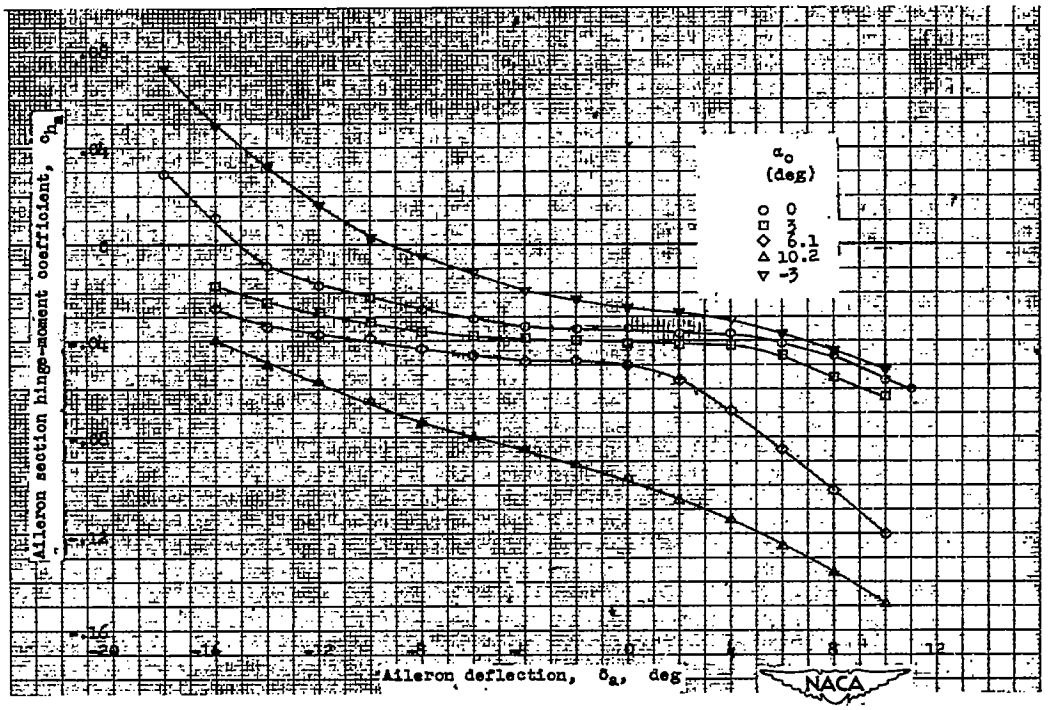

Figure 7.- Aileron section hinge-moment characteristics of the 0.20-chord true-contour aileron with sealed 0.50-aileron-chord internal balance on an approximate 0.178-chord-thick NACA 6-series-type airfoil section. R, 2.5×10^6.

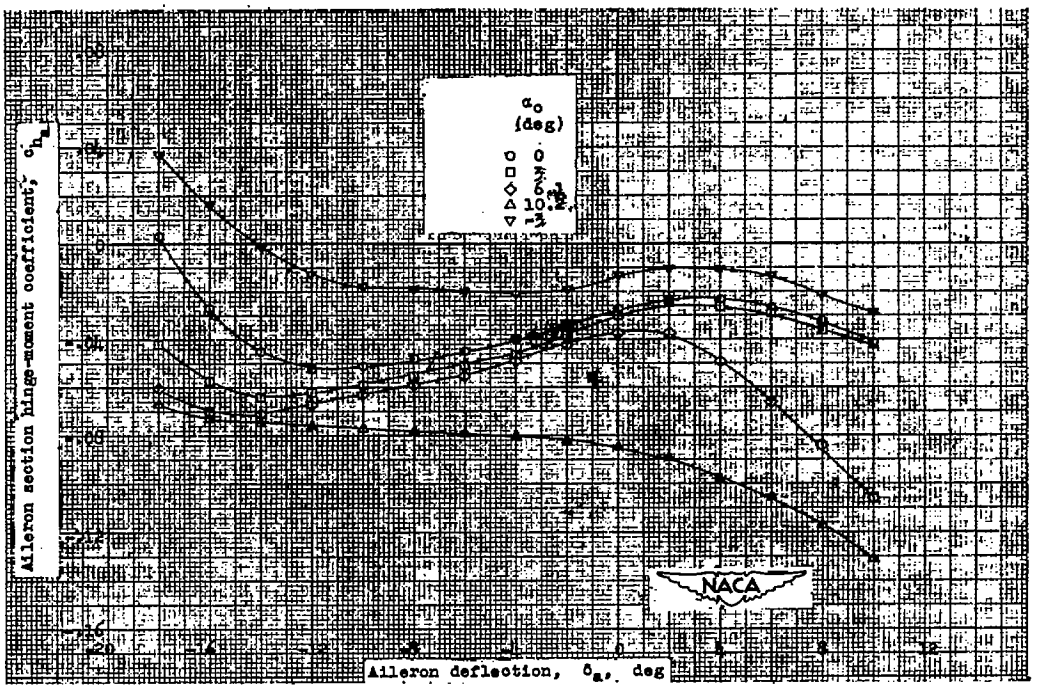

Figure 8.- Aileron section hinge-moment characteristics of the 0.20-chord true-contour aileron with sealed 0.60-aileron-chord internal balance on an approximate 0.178-chord-thick NACA 6-series-type airfoil section. R, 2.5×10^6.

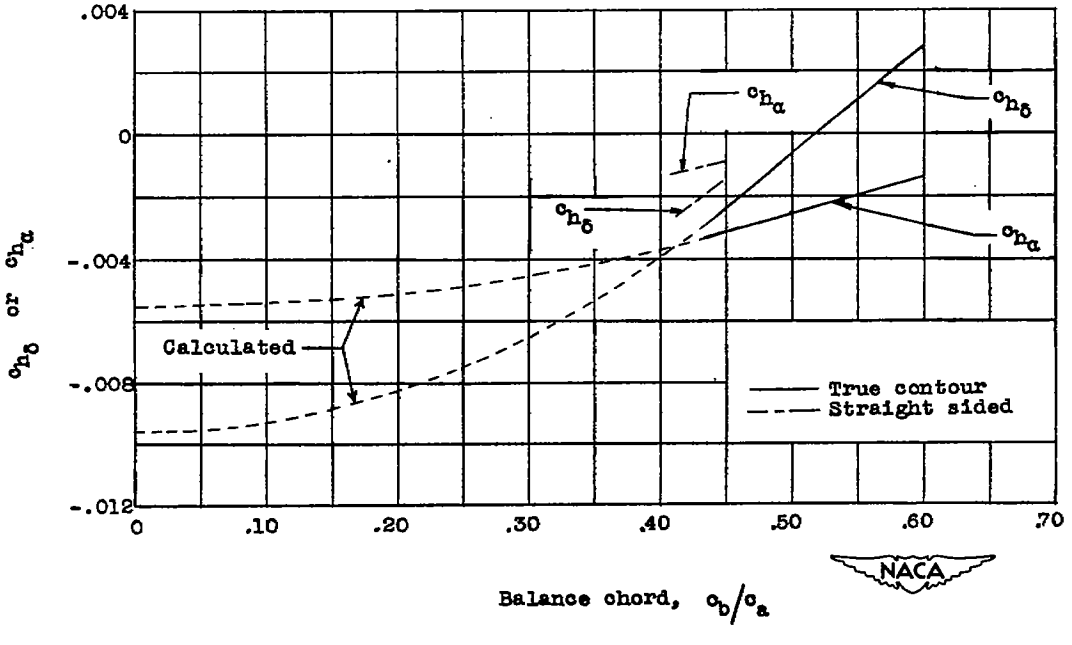

Figure 9.- The effect of sealed internal balance and aileron contour on the hinge-moment parameters c_{h_α} and c_{h_δ} of a 0.20-chord aileron on an approximate 0.178-chord thick NACA 6-series-type airfoil section. R, 2.5×10^6.

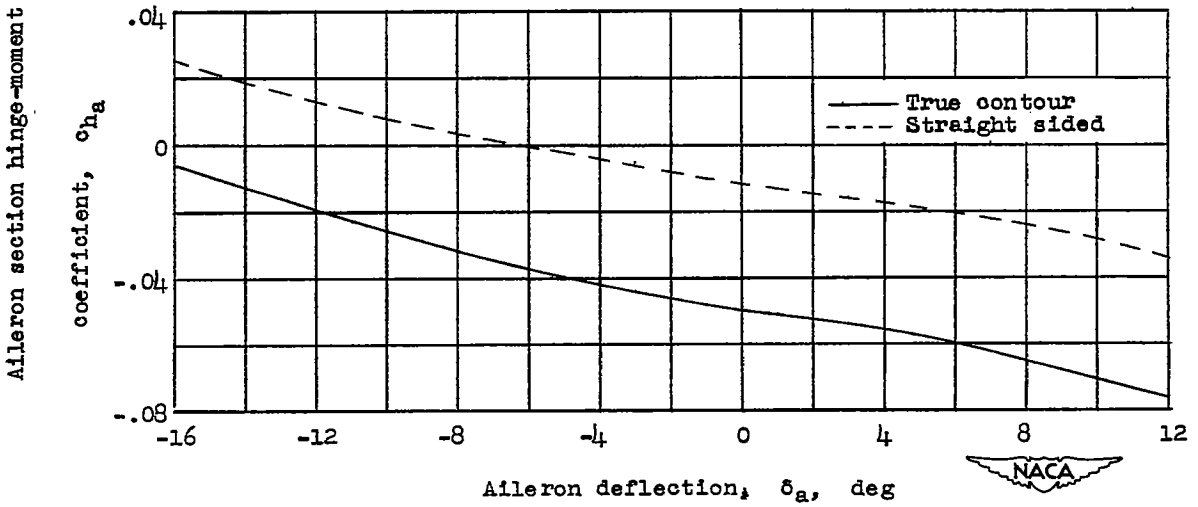

Figure 10.- Variation of aileron hinge-moment characteristics with aileron deflection at a constant section lift coefficient of 0.40 on an approximate 0.178-chord thick NACA 6-series-type airfoil section for two differently shaped 0.20-chord-ailerons with sealed 0.43-aileron-chord internal balance. R, 2.5×10^6.

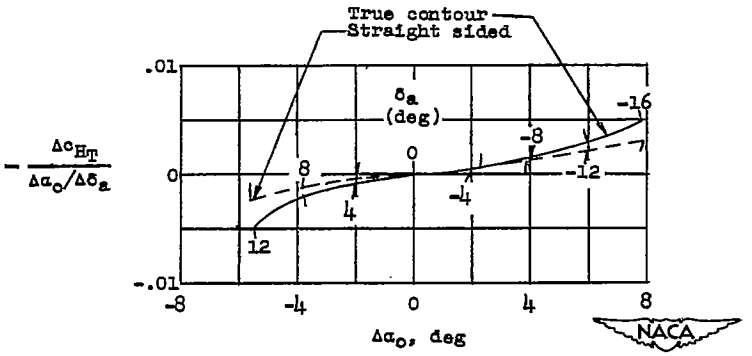

Figure 11.- Variation of the hinge-moment parameter $\frac{\Delta c_{H_T}}{\Delta \alpha_o / \Delta \delta_a}$ with equivalent change in section angle of attack required to maintain a constant section lift coefficient of 0.40 for deflection of differently shaped 0.20-chord ailerons with sealed 0.43-aileron-chord internal balance on an approximate 0.178-chord-thick NACA 6-series-type airfoil section. R, 2.5×10^6.

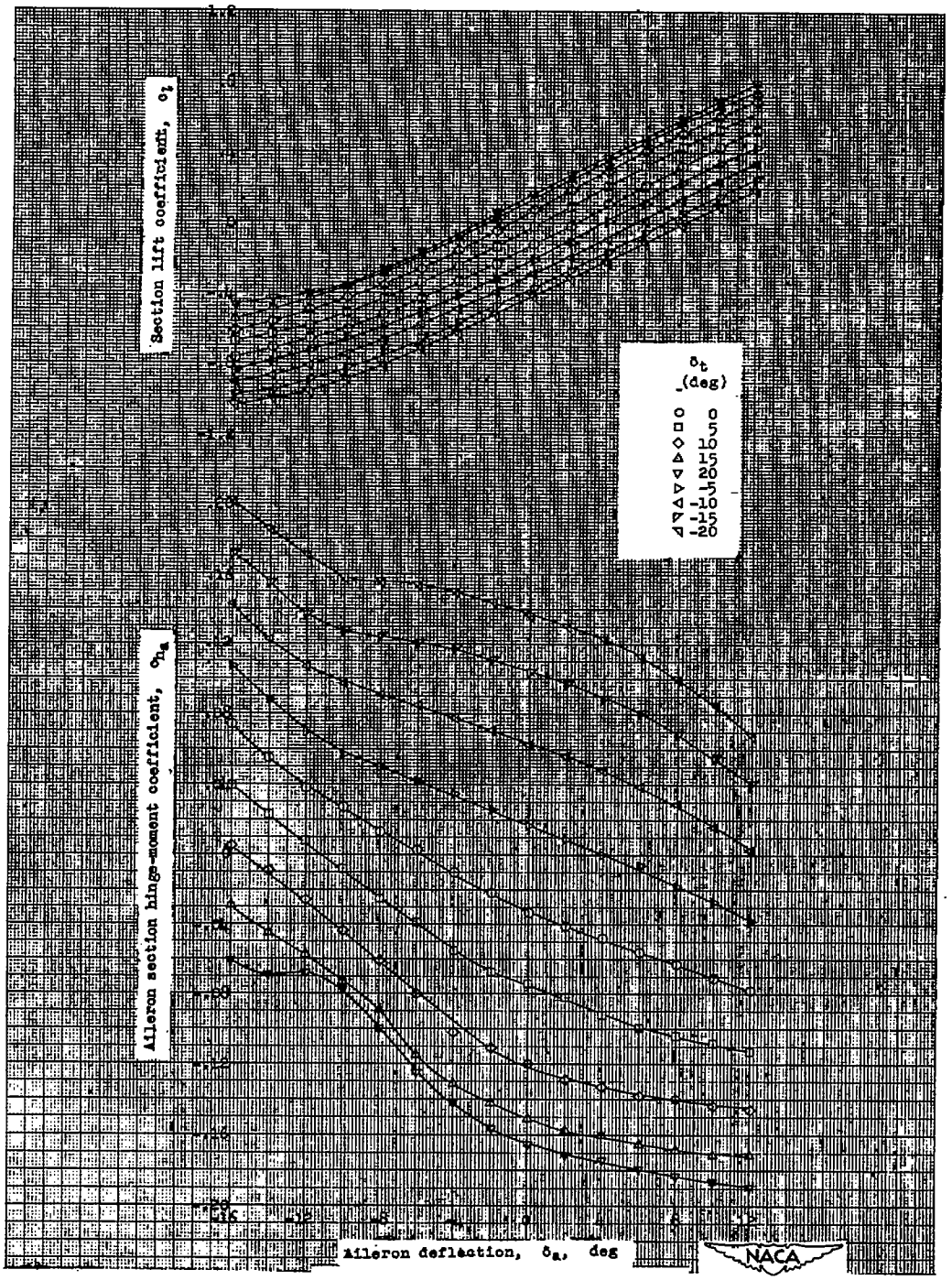

(a) $\alpha_o = -3^\circ$.

Figure 12.- Aileron effectiveness and hinge-moment characteristics of the 0.20-chord true-contour aileron with sealed 0.43-aileron-chord internal balance and with a 0.05-chord tab on an approximate 0.178-chord-thick NACA 6-series-type airfoil section. R, 2.5×10^6.

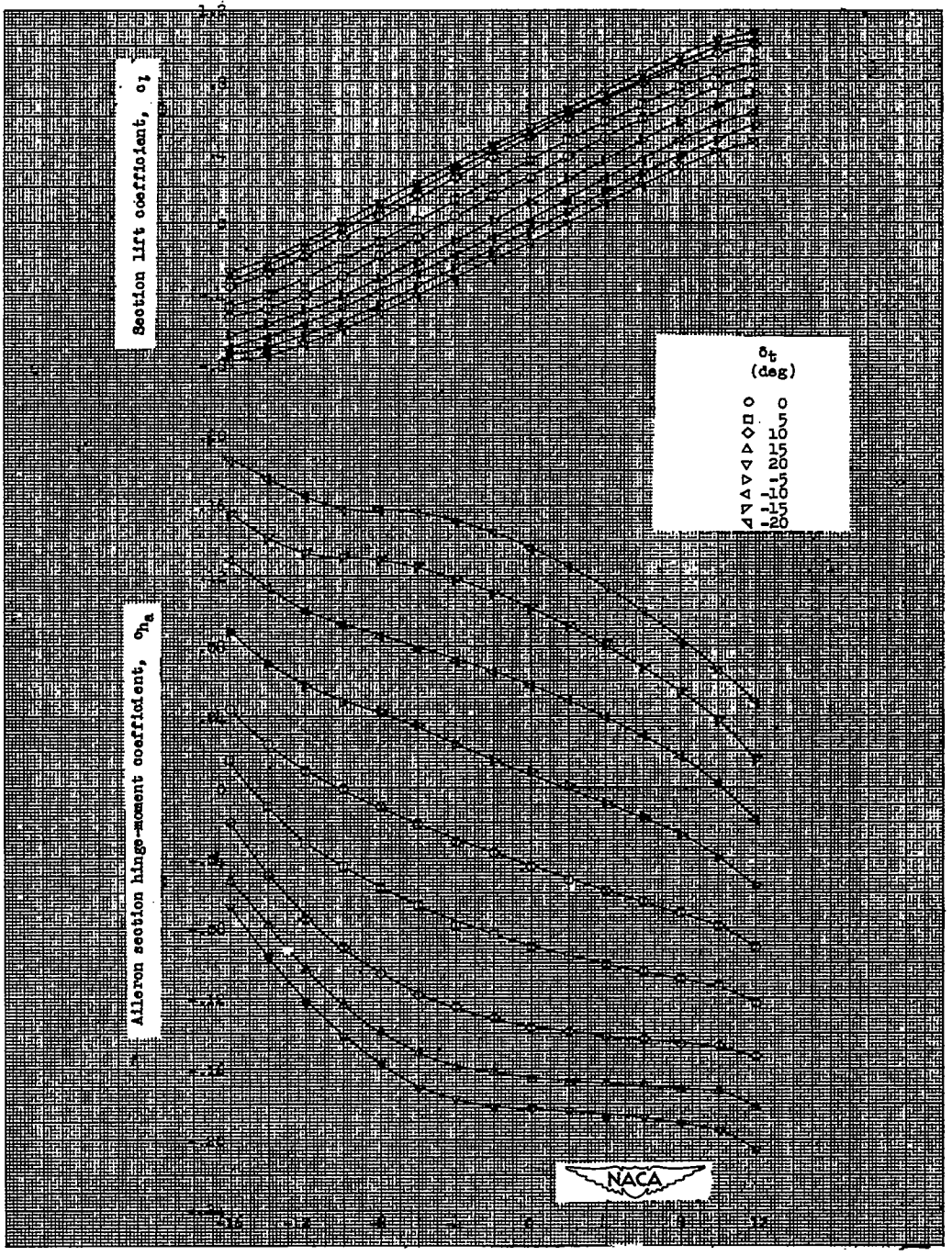

(b) $\alpha_o = 0°$.

Figure 12.- Continued.

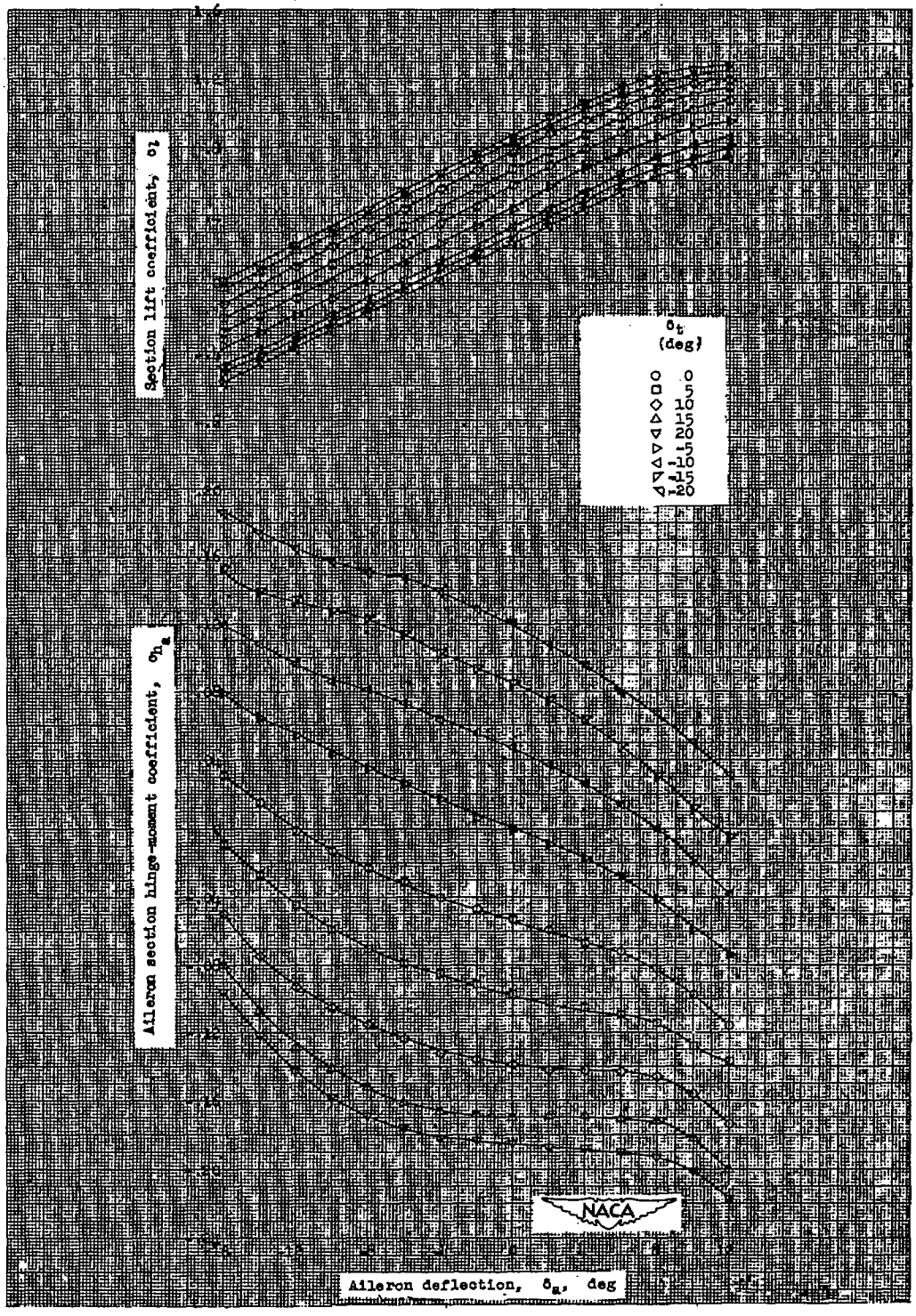

(c) $\alpha_0 = 3°$.

Figure 12.- Continued.

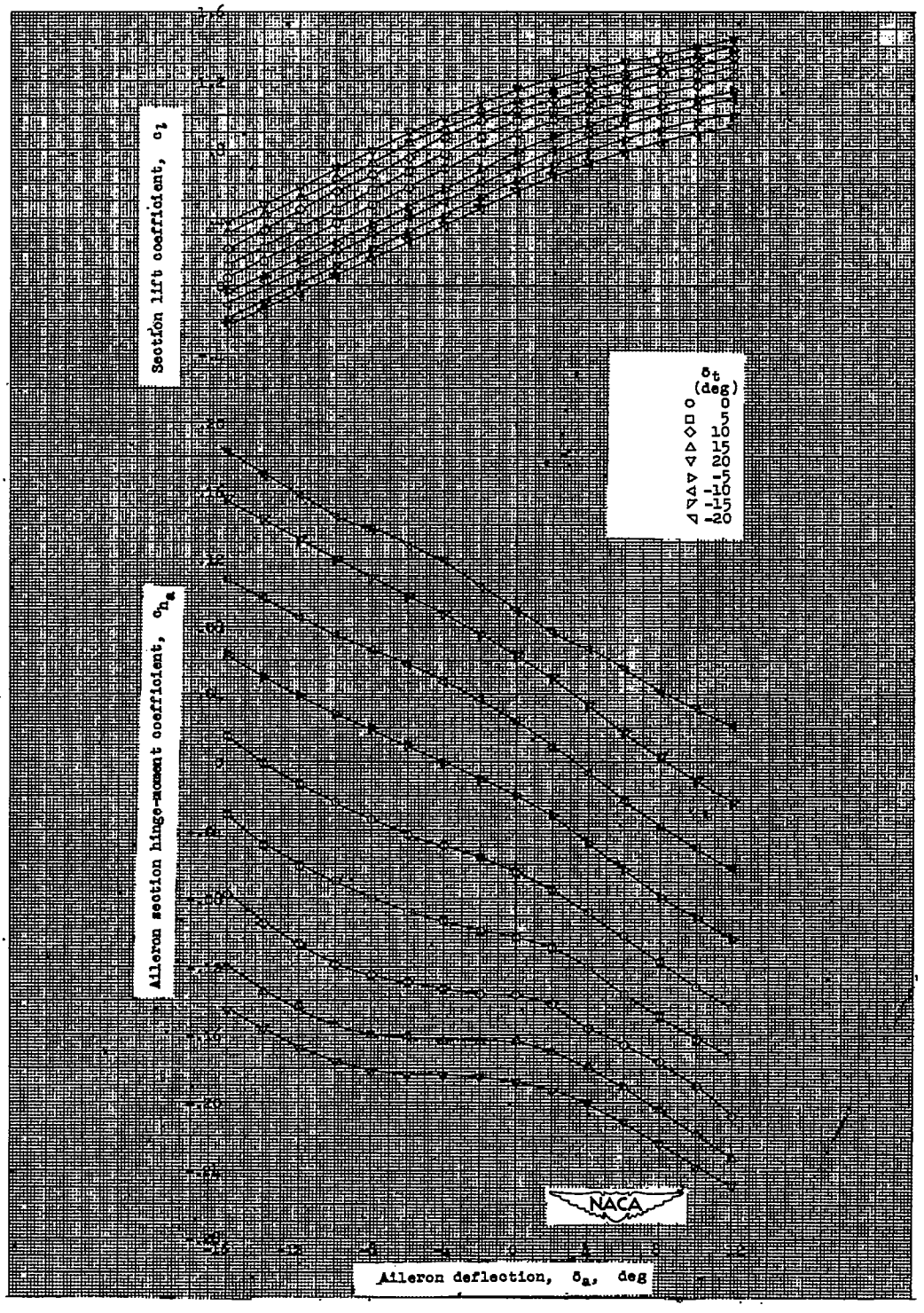

(d) $\alpha_o = 6.1^\circ$.

Figure 12.- Continued.

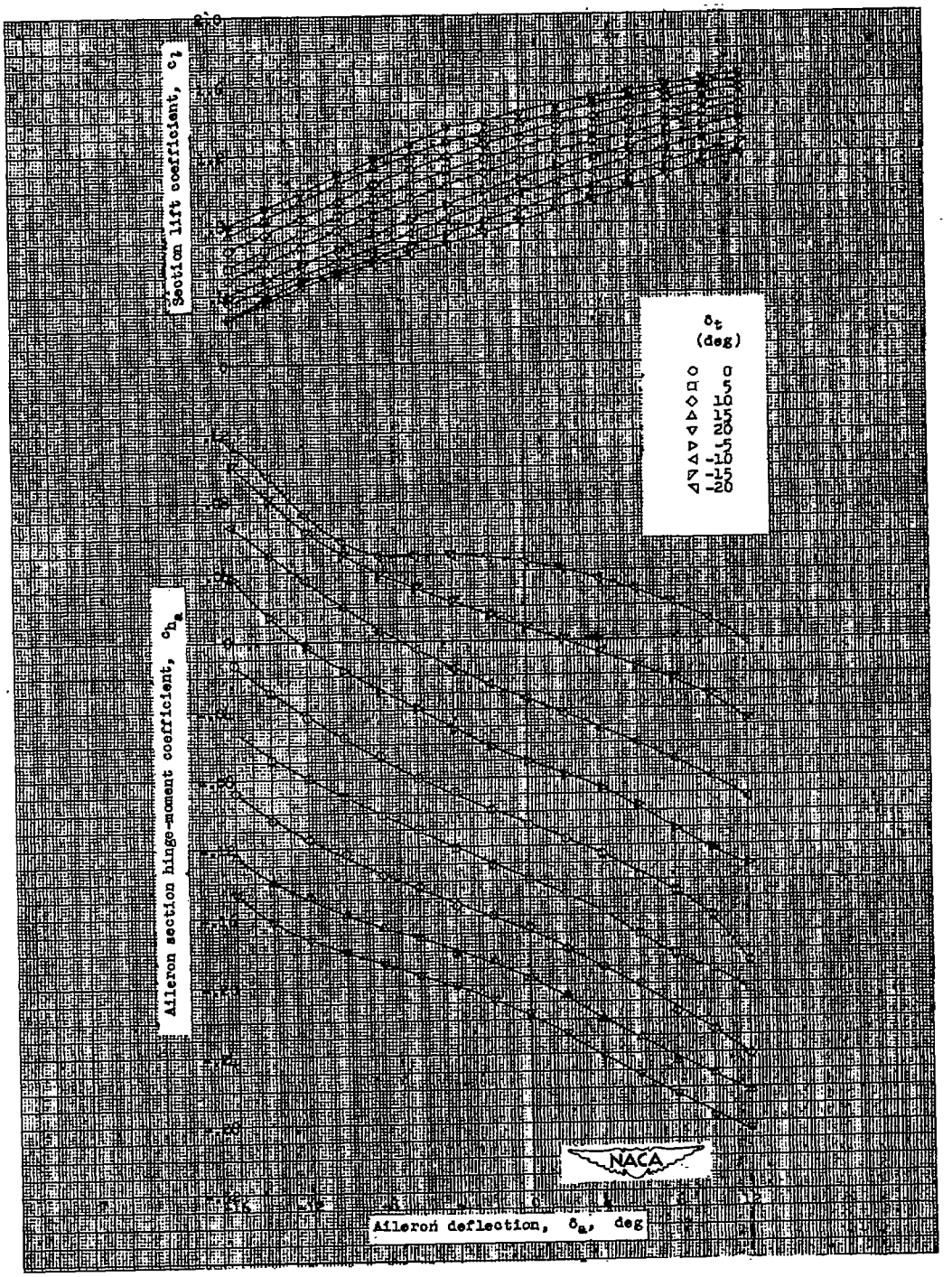

(e) $\alpha_o = 10.2°$.

Figure 12.- Concluded.

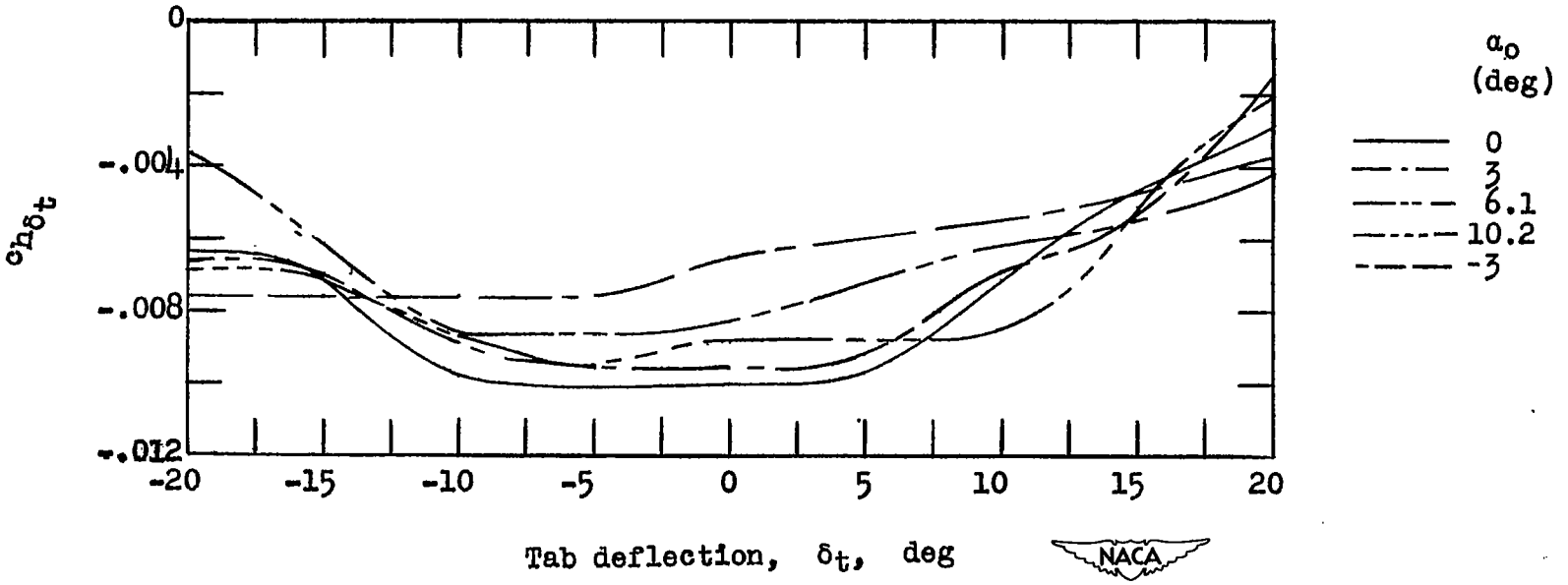

Figure 13.- Variation of the $c_{h_{\delta_t}}$ parameter with tab deflection for a 0.20-chord true-contour aileron with sealed 0.43-aileron-chord internal balance and with a 0.05-chord tab on an approximate 0.178-chord-thick NACA 6-series-type airfoil section. δ_a, 0°; R, 2.5×10^6.

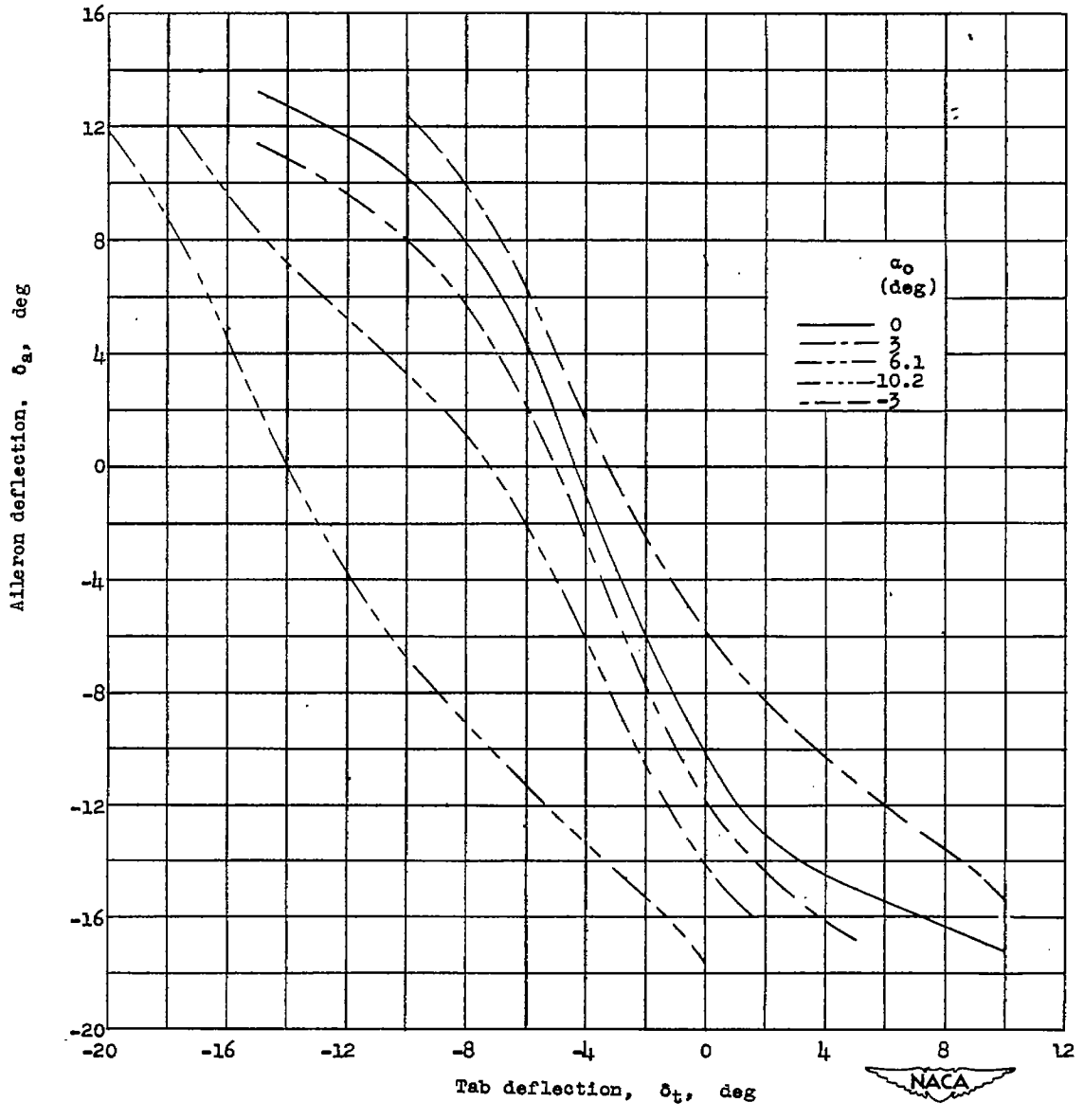

Figure 14.- Variation of aileron deflection with the tab deflection required to maintain a constant aileron section hinge-moment coefficient of zero on an 0.20-chord true-contour aileron with sealed 0.43-aileron-chord internal balance and with a 0.05-chord tab on an approximate 0.178-chord-thick NACA 6-series-type airfoil section. R, 2.5×10^6.